*Journal of Structural Geology*, Vol. 6, No. 1/2, pp. 39 to 49, 1984
Printed in Great Britain

0191-8141/84 $03.00+0.00
Pergamon Press Ltd.

# Obduction-related planar and linear fabrics in Oman

A. MICHARD*, J. L. BOUCHEZ† and M. OUAZZANI-TOUHAMI*

* Institut de Géologie, Université Louis Pasteur, 1, rue Blessig, 67084 Strasbourg, France; † Laboratoire de Tectonophysique, Université de Nantes, 2, rue de la Houssinière, 44072 Nantes, France

(*Accepted in revised form* 29 *July* 1983)

**Abstract**—Under the Oman ophiolites, three different types of Alpine, synmetamorphic fabrics are seen. Each of them is taken as the signature of a particular stage of the obduction process. The complex, high-grade fabric in the basal metamorphic sheet is linked to the intraoceanic detachment stage (pre-obduction *sensu stricto*). The $L + S$ fabric of the Muscat nappes and Hatat internal border, associated with low temperature, high pressure metamorphism, is regarded as the effect of an early obduction, that is the epicontinental thrusting of the Matrah peridotites. The much simpler fabric of the anchizonal Hawasina and autochthonous cover resulted from the gravity sliding of the Semail ophiolites during the final obduction phase.

## INTRODUCTION AND GEOLOGIC SETTING

LITTLE is known about obduction and still less about obduction-related fabrics. Thrusting of ophiolites upon continental crust (obduction *sensu stricto*) looks like a scandalous exception to the subductive fate of the oceanic lithosphere. Several geodynamic models have been elaborated to account for this phenomenon (Coleman 1971, 1981, Dewey 1976, Elliot 1976, Brookfield 1977, Parrot & Whitechurch 1978, Nicolas & Le Pichon 1980), but generally the accurate control that obduction-related structures and fabrics may offer has not been used. In this paper we wish to contribute to the understanding of the obducting process by the description of its structural signature in Oman (Fig. 1). This part of the Tethyan belt is particularly convenient for this purpose, since no collision succeeded the late Cretaceous obduction upon the Arabian platform. Moreover, the overall geology of the area is fairly well known since the work of Glennie *et al.* (1974). Figures 1 and 2 show the major units that classically constitute the Oman mountains, namely: the Arabian autochthonous terranes, the pelagic and volcanic Hawasina nappes, the Semail ophiolites including their basal sheet of metamorphic slices and the Late Maestrichtian-Tertiary cover. Two new items of data are also represented: first the Palaeozoic (Variscan?) synfolial folding of the pre-Permian autochthonous terranes (Lovelock *et al.* 1981, Michard 1982) and, second, the presence of a set of infra-ophiolitic metasedimentary nappes on the inner margin of the Saih Hatat window, that is the Muscat nappes (Boudier & Michard 1981, Michard 1983). The following is relative to the Alpine obduction-related structures in the four major infra-ophiolitic units namely the Permo-Mesozoic autochthonous cover, the Hawasina nappes, the Muscat nappes and the Semail basal metamorphics. We shall first consider the fabrics in the classical succession: autochthon–Hawasina–Semail, which is an *external* succession according to the vergence of the nappes, and then the fabrics in the *internal* Muscat nappes.

## THE FABRICS IN THE EXTERNAL TECTONIC PILE

The fabrics were observed in the four main windows that are eroded through the Semail nappe, namely on the southern edge of the Saih Hatat, on the northern border of the J. (Jabal) Akhdar–J. Nakhl, along the Wadi Hawasina and in the Sumeini sections (Fig. 1).

### *The Permo-Mesozoic autochthonous cover*

An incipient cleavage appears just under the nappes in the Muti marls (Campanian) and, in some places,

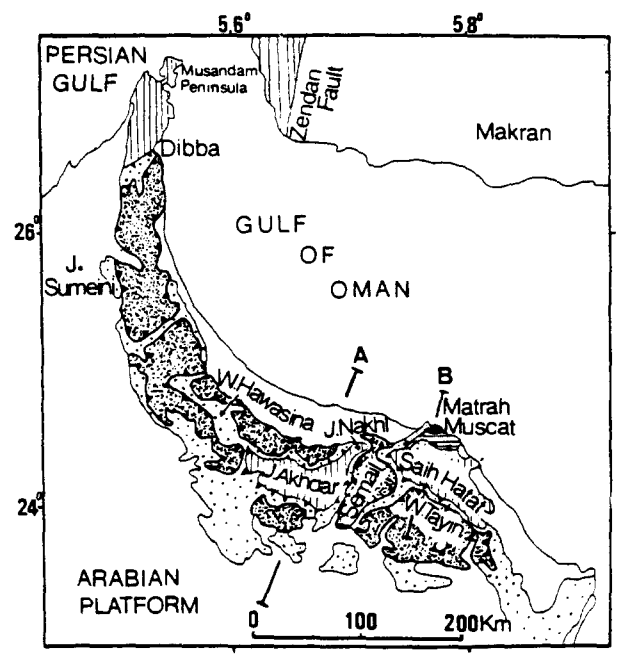


Fig. 1. Index map showing the main units of the Oman mountains and the principal geographical locations. *Dense stipple*, ophiolites; *light stipple*, Hawasina nappes and mélange; *vertically ruled*, autochthonous windows; *horizontally ruled*, Muscat nappes; *blank*, Late Maestrichtian–Tertiary cover (folded and non-folded) and Quaternary sands. After Coleman (1981), except for the Muscat-Saih Hatat area. *A*, location of the main part of the profile shown in Fig. 2; *B*, approximate location of the 'unfolded' profile shown in Fig. 16. The innermost part of this 'B' profile is hypothetically projected onto the A profile (Fig. 2).

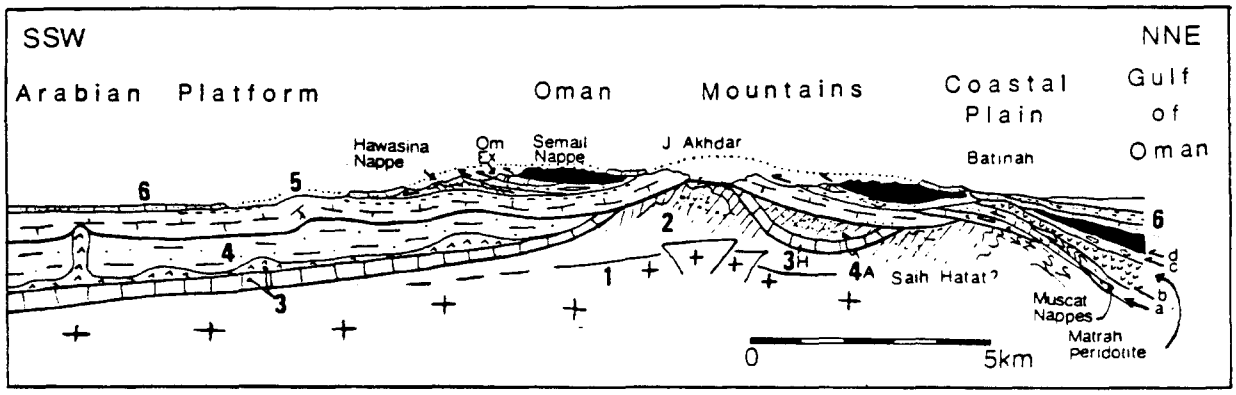


Fig. 2. Schematic geological profile of the Oman belt (Arabian foreland stratigraphy and Oman Mountains nappes after Glennie 1977). Palaeozoic folding of the Jabal Akhdar window and innermost tectonic pile of the Muscat area (which is hypothetically projected into this profile) after Michard (1983). For location see Fig. 1. 1, Precambrian basement (Panafrican belt); 2, Late Proterozoic terranes, affected by a Palaeozoic epizonal folding; 3, Eocambrian–Early Cambrian stromatolitic limestones and Early Cambrian salt (Arabian platform) (3H—Hijam and Kharous formations); 4, Middle to Late Cambrian, Ordovician and Silurian terrigeneous formations (4A—Amdeh quartzite and schists, with Ordovician fossils); 5, Permian to Late Cretaceous calcareous cover of the Arabian platform and Oman Mountains autochthon. Its uppermost part (Campanian–Early Maastrichtian, Muti Marls) is indicated by a dashed line; 6, Late Maastrichtian–Tertiary neoautochthonous cover (laterites and basal conglomerates, calcarenites).

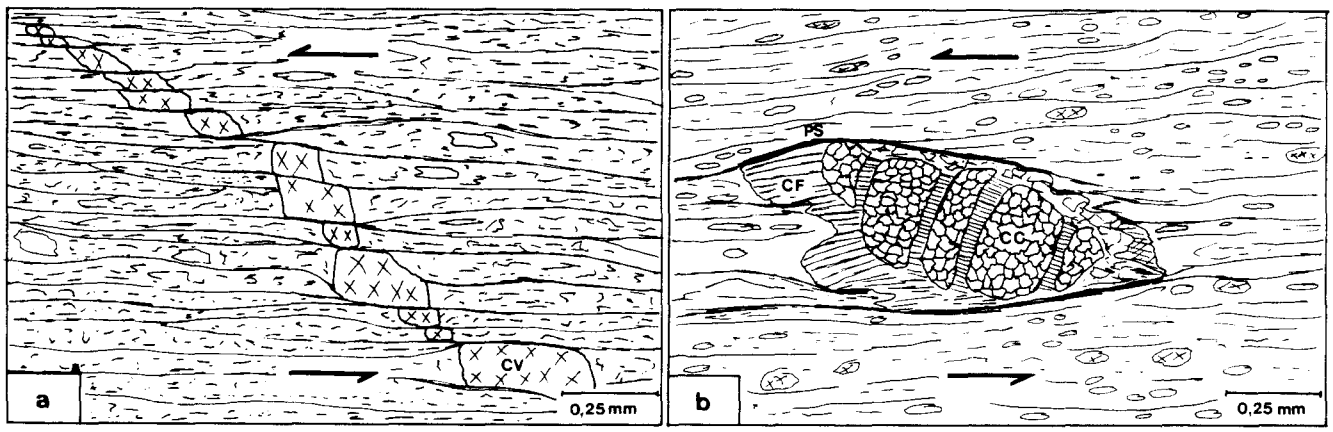


Fig. 3. Microstructures in the autochthonous Muti Marls just below the nappes, Wadi Tayin area—*XZ* sections. (a) Dissolution cleavage and shearing: the fragments of an early calcite vein (CV), although originally perpendicular to cleavage are offset due to shearing along the cleavage planes. (b) Pressure solution (PS) and boudinage oblique to the cleavage and asymmetric pressure shadows (CF, calcitic fibres) associated with a calcareous clast (CC) indicate the same shearing direction.

among the limestones underneath. This cleavage nearly parallels the bedding. It is a spaced dissolution cleavage (Figs. 3a & b) which locally bears a stretching lineation directed N 10 to 40°E. This lineation is related to some plastic deformation in the limestones as shown by the flattened and stretched calcareous pebbles (Figs. 3b and 4a) and by extensional gashes (Fig. 4b), perpendicular to the N 10–40°E direction. Plastic deformation, accompanied by some shearing parallel to cleavage which offsets calcite veins (Fig. 3a), is attributed to the emplacement of the nappe.

The latter interpretation is supported by some major structures that are observed in the J. Nakhl area. There, the top part of the Permo-Mesozoic limestones is truncated by low-angle bedding faults (Fig. 4e), while their base, normally discordant on the Proterozoic–Palaeozoic slate belt, is converted into a décollement fault with minor, recumbent, N 50–80°E trending folds, associated with a N 0–30°E stretching lineation (Fig. 4d).

According to an illite crystallinity study in the Campanian marls of the Wadi Tayin area, the syntectonic metamorphism just reached the anchizonal grade in this central part of the autochthon.

*The Hawasina nappes and mélange*

Penetrative deformation remains weak in these units. Now, the cleavage parallels the axial plane of $F_1$ folds that are well developed, probably due to the highly stratified nature of the pelagic series. The type and dip of the cleavage both change with position in the belt. In relatively external positions (Sumeini), a steeply dipping fracture cleavage is seen, associated with westward-verging open folds (Fig. 5a). In more central positions (Wadi Hawasina, J. Nakhl, Wadi Tayin), where illite crystallinity attains the lowest anchizone a flat and usually refolded penetrative cleavage is found (Fig. 5b), occasionally associated with a poorly marked stretching lineation close to N 20°E.

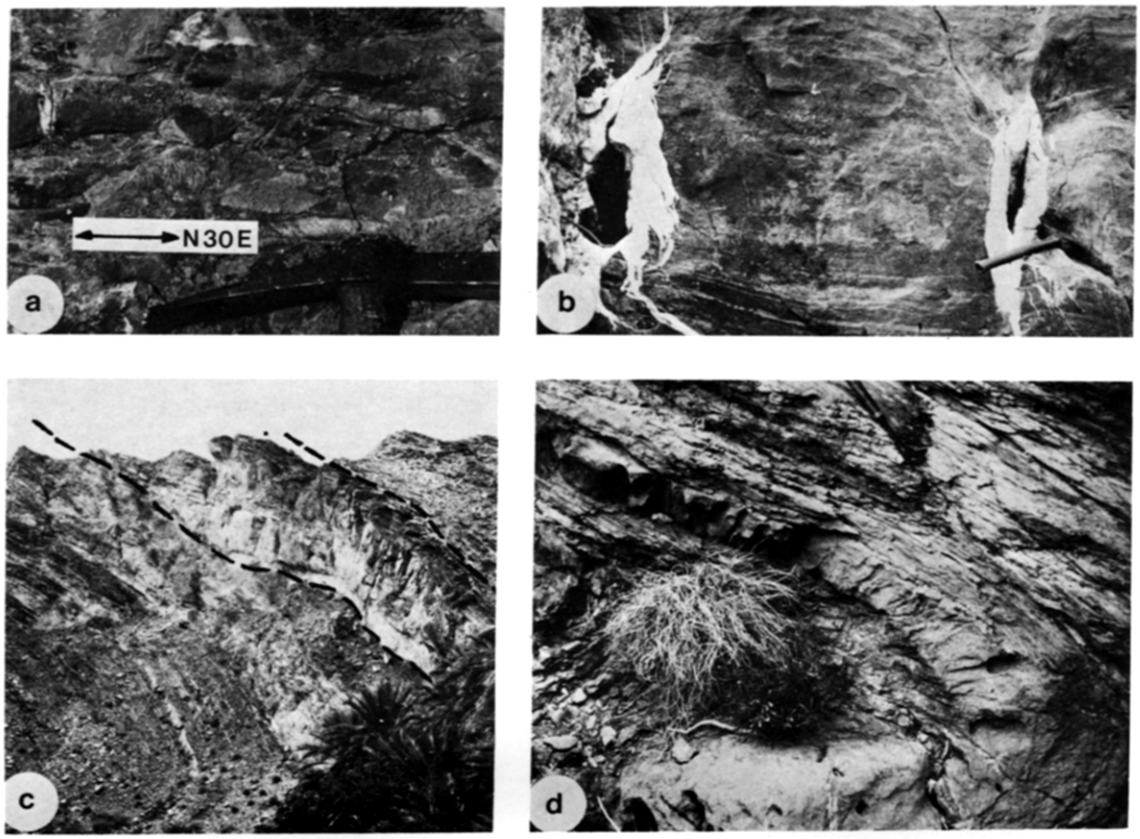


Fig. 4. Deformation of the autochthonous limestones, Jabal Nakhl area. (a) Stretched calcareous pebbles as seen on the top of a Cretaceous conglomeratic limestone, a few metres below the base of the nappes; southeastern limb of the J. Nakhl anticline. (b) Incipient necking and boudinage of a siliceous limestone bed within the Cretaceous series; northwestern limb of the J. Nakhl anticline. The tension gashes are nearly vertical and directed N 130°E. (c) Low-angle fault in the upper beds of the Jurassic limestones *(JL)*, below the Hawasina mélange *(HM)*; northwestern limb of the J. Nakhl anticline. (d) Drag folds in the lowermost beds of the Permian limestones, detached from the Proterozoic–Palaeozoic basement of the J. Nakhl anticline. The axes of the drag folds trend N 50–80°E; pressure shadows against pyrites stretch N 0–30°E, parallel to the hammer handle.

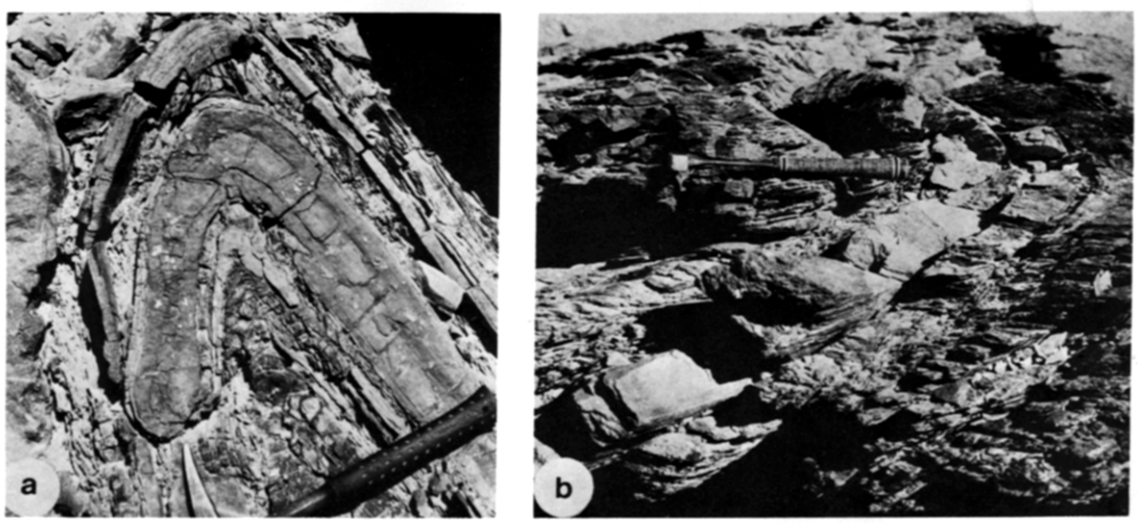


Fig. 5. Folds and cleavage in limy turbidites from the Hawasina nappes. (a) Incipient fracture cleavage in upright folds; external Hawasina, Sumeini section. (b) Slaty cleavage in recumbent $F_1$ folds (refolded by major $F_2$ folds); Hawasina window.

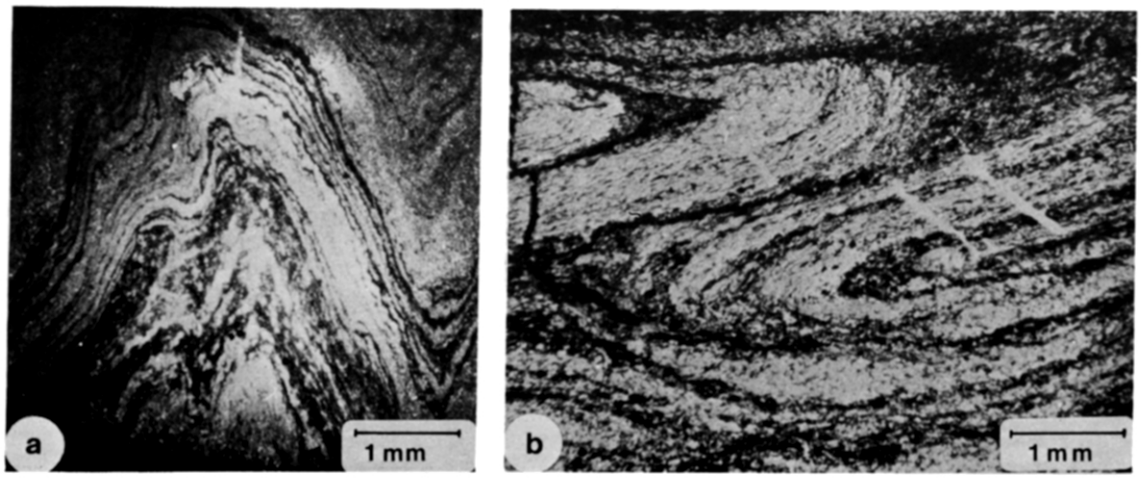


Fig. 6. Microstructures in the infra-ophiolitic metamorphic slices; Wadi Tayin area. (a) Open strain–slip ($F_3$) folds in the greenschists. (b) Intrafolial folds ($F_2$) in the amphibolites.

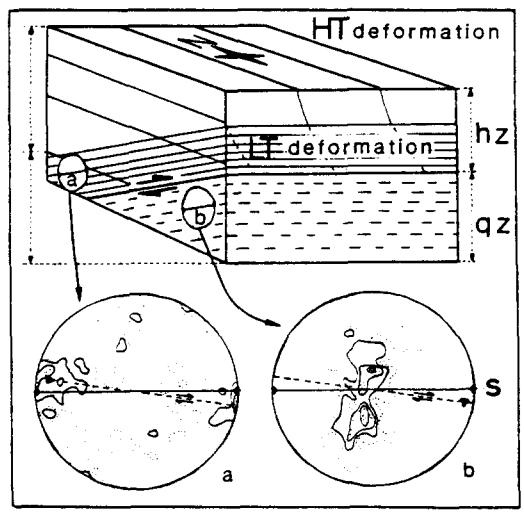


Fig. 7. Relationship between deformation in the harzburgites (hz) and in the quartzites (qz) in the Semail ophiolite, after Boudier *et al.* (1982). (*a*) and (*b*) are equal-area lower-hemisphere projections of crystallographic axes, respectively [001] orthopyroxene slip direction in peridotite mylonite and [0001] quartz axes in quartzite layers. 100 measurements. *XZ* finite strain reference system: the solid horizontal line is parallel to the lineation and to the trace of the foliation. The flow plane (dashed line) and the sense of shear (double arrow) are identical in both diagrams. The flow plane is deduced from the crystallographic axis distribution. The quartz *c*-axes distribution is consistent with a high temperature deformation (prismatic and/or rhomb slip; discussed *in* Bouchez & Pêcher 1981). High temperature flow plane (mantle history; steeply dipping plane) is not considered here.

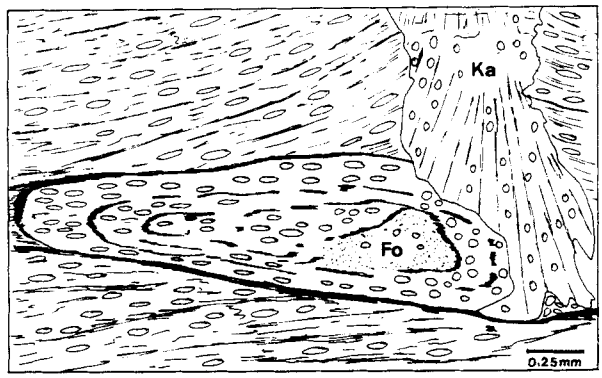


Fig. 10. Heterogeneous flattening around an early fan of Fe–Mg carpholite (Ka); detrital layer within the Ruwi limestones. The ferrugineous oolithic spot (Fo) is less flattened close to the fan than outside it. The quartz clasts preserve their equiaxial shape in the poecilitic carpholite as well as in the ferrugineous spot close to it; they are flattened elsewhere. The cleavage is deflected around the cluster.


Fig. 11. The strong stretching lineation of the Hatat metamorphics, observed on a foliation surface gently dipping towards the south. Compass (bottom) is 15 cm long.

We admit that these deformations and weak recrystallizations, which closely resemble those of the autochthon, also originate from shearing due to the overriding ophiolites. Hence the latter fabric variations may be explained by the change in thickness of the Semail nappe. But it is remarkable to note that the Hawasina mélange which crops out just west of Matrah–Muscat (Darsayt, Medina Quaboos), hence in an internal position (Figs. 1 and 8) does not show any cleavage associated with its clearly visible recumbent isoclinal folds. We conclude that these Hawasina series rocks never carried a thick ophiolite overburden, a deduction which is in agreement with their position above the Matrah peridotite (Michard 1983).

*The Semail basal sheet*

Contrasting with the underlying Hawasina and autochthonous low-grade units, the Semail basal sheet is composed of discontinuous slices of high- and medium-grade materials: amphibolites with marbles and piemontite–quartzites; greenschists with albite–amphibolites, porphyroids and quartzites. Considered as oceanic crustal materials since the publication of Glennie *et al.* (1974), they were subject to recent petrographic and isotopic investigations in order to decipher the earliest 'detachment' stage of the forthcoming obduction (Searle & Malpas 1980, Coleman 1981, Ghent & Stout 1981).

Despite the large movements associated with the final phase of thrusting onto the Hawasina nappes and the Arabian platform, these slices retain some structural record from their earlier intra-oceanic formation. In the lowest slices, belonging to the greenschist facies, many intrafolial folds can be recognized, suggesting that the present foliation transposes earlier ones. In some places the foliation is clearly refolded by asymmetric strain-slip folds (Fig. 6a) which geometrically correspond to the earliest $F_1$ folds of the Hawasina series (Wadi Tayin). Closer to the peridotites, the highest slices, of amphibolite metamorphic grade, have a strong planar fabric which also shows a complex history (Fig. 6b). Due to the competence of these rocks and of the overlying peridotites, late-fold events scarcely appear. The stretching or mineral lineations imprinted on the foliation planes are variously oriented depending on the metamorphic grade (related to position within the sheet), reflecting reorientation as well as successive generations. At the scale of the whole belt, the average orientation of the lineations depends on the geographical position: N 0–2°E in the north (Sumeini), N 160 E–N 0° in the central part (Wadi Hawasina) and N 60–120°E in the southern part (J. Nakhl and Wadi Tayin). This is interpreted as a change in orientation of the intra-oceanic thrusting which, moreover, was not synchronous everywhere (propagating from south to north; Misseri 1982). The structures which we recorded, at least those imprinted on the higher grade part of the metamorphic sheet, closely correspond to the mylonitic 'low temperature' structures of the lowest part of the overlying peridotites

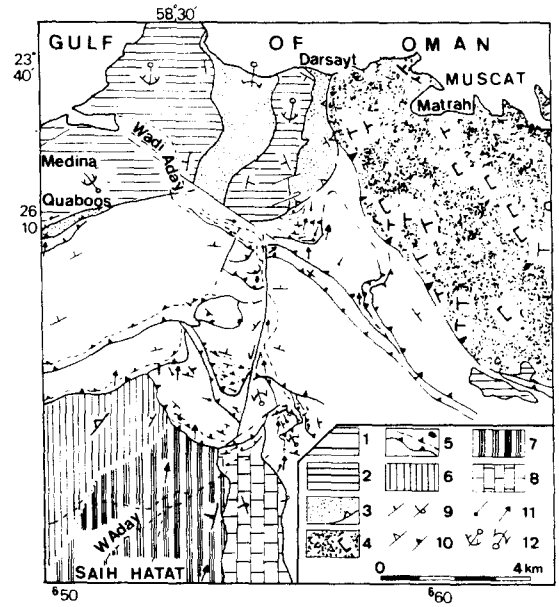


Fig. 8. Structural map of the Muscat area, after Michard (1982b). 1, Plio-Quaternary sands of the Batinah coast; 2, Late Maestrichtian–Tertiary neo-autochthonous cover; 3, Hawasina mélange; 4, Matrah peridotites (with orientations of dunite banding and harzburgite foliation according to Boudier & Nicolas, pers. comm.); 5, Muscat nappes, with major and secondary synmetamorphic thrust planes, black dot near Douar Wadi (DWA); serpentinites; 6, Late Proterozoic greywackes affected by Palaeozoic folding (Hatat greywackes); 7, the same, affected by Alpine metamorphism (Hatat metamorphics); 8, Early Cambrian limestones (Hijam formation), metamorphosed together with the Hatat schists; 9, bedding dips (normal & inverted); 10, foliation dips (Hercynian & Alpine) in Saih Hatat; 11, Synmetamorphic folds axes and stretching lineations; 12, Tertiary fold axes (syncline & anticline).

(Boudier & Coleman 1981, Misseri 1982). The lattice fabric measurements in the quartzites associated with the amphibolites indicate a dominant simple shear regime with the same sense as in the olivine rocks (Fig. 7) (Boudier *et al.* 1982). Hence, both mesoscopic and microscopic fabrics developed during the intra-oceanic 'detachment' process.

## THE FABRICS IN THE INTERNAL TECTONIC PILE

*General characters*

We now consider the northeastern Saih Hatat–Muscat area, which is the innermost part of the Oman mountains (Figs. 1 and 8). There, the base of the tectonic pile consists of a part of the Arabian basement (NE-Saih Hatat window) which is metamorphosed. It is overlain by the Muscat nappes, made of metamorphosed Proterozoic to Mesozoic terrains, which in turn are overlain by the Matrah peridotites along their eastern margin. Finally, the Hawasina mélange is tectonically discordant upon the Matrah peridotites and the Muscat nappes (Michard 1983). The structural characters of the Hawasina mélange in this area have been described above. Structural analysis of the Matrah peridotites is still in progress (Nicolas and Boudier, pers. comm), but the porphyroclastic microstructures and the dunitic

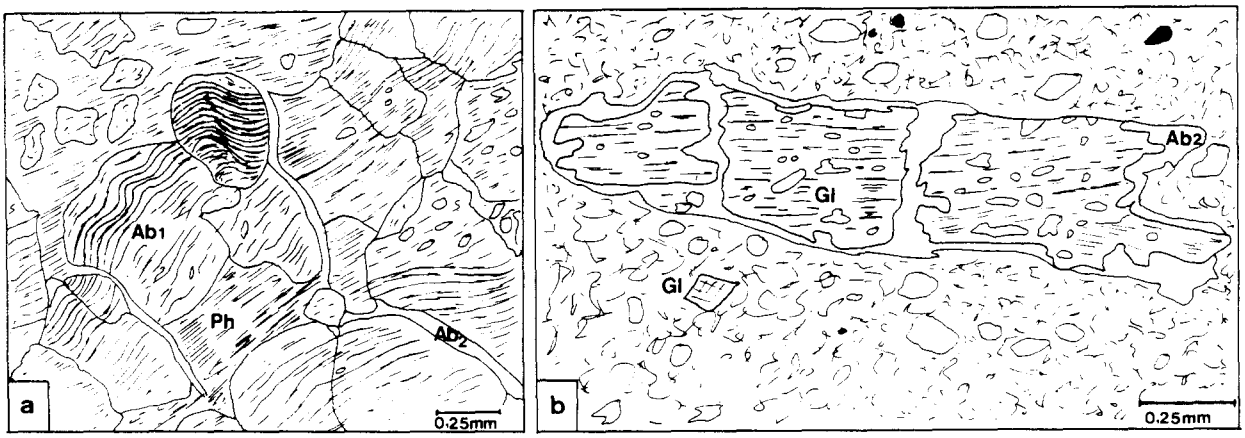


Fig. 9. Microstructures in the HP–LT metamorphics, with indications of late syncrystallization stretching. (a) Hatat schists. The early albite poeciloblasts (Ab1) incorporate an earlier and already deformed foliation, parallel to the surrounding phengite crystals (Ph). The Ab1 crystals are disrupted by late albite gashes (Ab2) growing perpendicularly to the stretching direction. (b) Wadi Aday metavolcanites (Muscat nappes). The large crossitic glaucophane crystal (G1) is crosscut by tension gashes infilled by late albite (Ab2) which also constitutes a reactional rim and pressure shadow around the early glaucophane.

banding parallel to the rock foliation suggest that they were deformed in an intra-oceanic thrusting environment. In that sense, and despite the lack of observed mylonitic microstructures which are usually encountered at the extreme base of the Semail peridotites, the Matrah peridotites can also be considered as 'basal' peridotites. Their banding (and foliation) is gently to moderately dipping to the NE and the average direction of the tectonic lineation is E–W, which is conformable with the shear direction described in the Semail basal peridotites of the Wadi Tayin area (Boudier & Coleman 1981).

The Muscat nappes and the northeastern Saih Hatat area will be described together, both having the same structural and metamorphic patterns. They are characterized by a syntectonic metamorphism, initiating in the blueschist facies (with glaucophane, Fe Mg—carpholite, and lawsonite) and terminating in the upper greenschist facies (Michard *et al.* 1981, Boudier & Michard 1981, Michard *et al.* 1982, Michard 1983, Lippard 1983, Michard *et al.* 1983). The age of this HP–LT metamorphism is post-Triassic since it affects Triassic dolostones in the Muscat nappes, which even include fossiliferous Permian limestones (Michard 1983, Vachard, pers. comm). Published K/Ar ages are scarce and dispersed, the youngest being close to 80 MA (Michard *et al.* 1982, Lippard 1983).

*The HP–LT foliation*

The fabric which developed during this HP–LT episode is of an '$L + S$' type. In the whole area which has been mapped (Michard 1983) the geometrical homogeneity is only locally disturbed by the lithological heterogeneities and by some of the major structures (wrench faults, competent mega-lenses). In the incompetent series, the main foliation is typically a penetrative secondary $S_2$ cleavage which transposes an earlier metamorphic one ($S_1$) and gently dips parallel to the late duplex fault planes. In the competent slabs (200–1000 m thick limestones and dolomicrites series), an apparently simple $S_1$ foliation is present; axial plane to some of the minor $F_1$ folds and parallel to the flat-lying bedding, except in the hinges of some major $F_2$ folds where a closely spaced crenulation cleavage has developed. The structures at the scale of the optical microscope (Figs. 9, 10 and 12) confirm that flattening and shearing, developed throughout the whole metamorphic evolution, are responsible for the main foliation of the rocks.

*The HP–LT lineation*

The foliation $S_{1-2}$ or $S_2$ bears a well-marked stretching lineation, which developed during the $F_2$ phase and affected the $F_{1-2}$ phenoblasts (Fig. 9). The lineation is ubiquitous in the Muscat nappes, with the exception of the competent dolomicrite layers, and is probably still more imprinted in their autochthonous sole, that is in the NE-Hatat metamorphics (Fig. 11). There, frequent tension-gashes were observed, widely opened perpendicular to the stretching direction and infilled with minerals of a quartz–albite–chlorite–phengite paragenesis. The same mineral association was observed in the pressure-shadows associated with the Fe–Mg carpholite, glaucophane, lawsonite or albite phenoblasts. This indicates that the fabric of the HP–LT metamorphics was achieved during the transition to the upper greenschist facies. Imprinted on the flat-lying foliation of the Hatat and Muscat schists, this lineation is constantly trending at N 10 ± 10°E over a large area (Fig. 8). Associated, at a larger scale, with the contemporaneous emplacement of the Muscat nappes, the rock fabric clearly developed in rotational shearing conditions. Microscopic observations in the $XZ$ plane frequently show asymmetric pressure shadows indicating a southward-directed thrusting (Fig. 12). A SSW-directed simple shear component of strain is also reflected in the quartz $c$-axis preferred orientations in some Hatat quartzites or quartz-rich rocks (Fig. 13). Finally, this fits with the vergence of the major folds in the Muscat nappes (Fig. 14) and with the

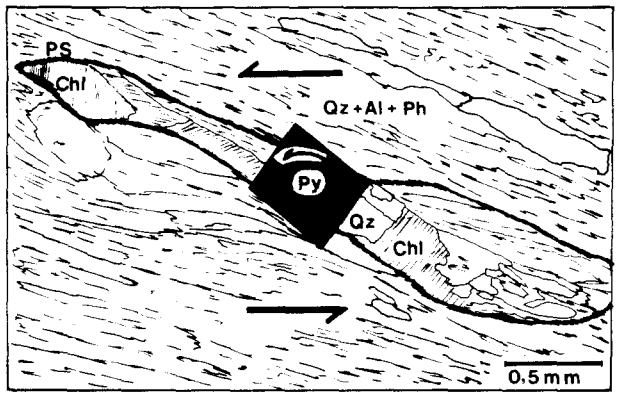


Fig. 12. Asymmetric pressure-shadow associated with a pyrite crystal (Py); Hatat schists. It indicates a rotational strain, at least during the latest crystallization. The shape of the quartz-chlorite shadow (Qz, Chl) and the location of the pressure solution zone (PS) give the sense of shear (double arrow) (see also Malavieille *et al.* 1982).

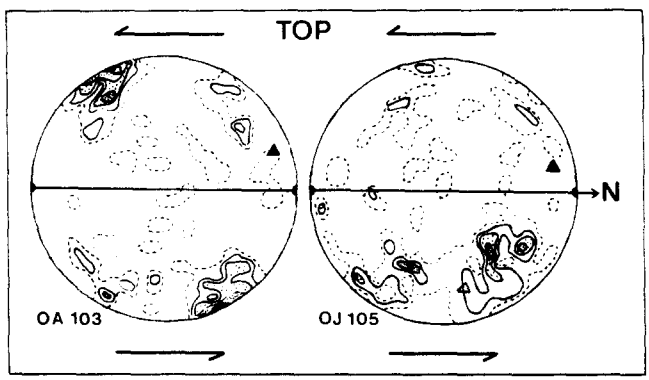


Fig. 13. Preferred orientation of quartz *c*-axes in a quartzite (OA 103) and a quartz-rich schist (OJ 105); NE Saih Hatat. Equal-area lower-hemisphere projection. 100 measurements. *XZ* finite strain reference system: solid line parallels the lineation and trace of foliation. Black triangle: computed pole of the girdle emphasizing the fabric asymmetry which gives the sense of shear (arrows). White triangle computed maxima of *c*-axes. In OA 103, basal slip predominates, indicating a low temperature deformation. The asymmetric distribution of *c*-axes in OJ 105 is not as obvious as in OA 103, probably due to a higher content in micas.

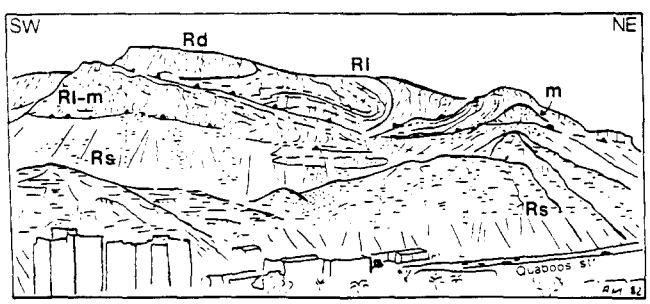


Fig. 14. Truncated recumbent folds and hectometric duplex in the Muscat nappes, NW Ruwi hills (as seen from the central Ruwi hill) (after Michard 1983). Rs, Ruwi phengitic schists; Rl, Ruwi Permian limestones (including Fe–Mg carpholitic layers, Fig. 10); Rd, Ruwi dolostones; m, mylonitic marbles (tectonic lenses). The axes of the main folds are trending N 60°E on the left, N 20°W on the right. The inverted limb is half the thickness of the normal one.

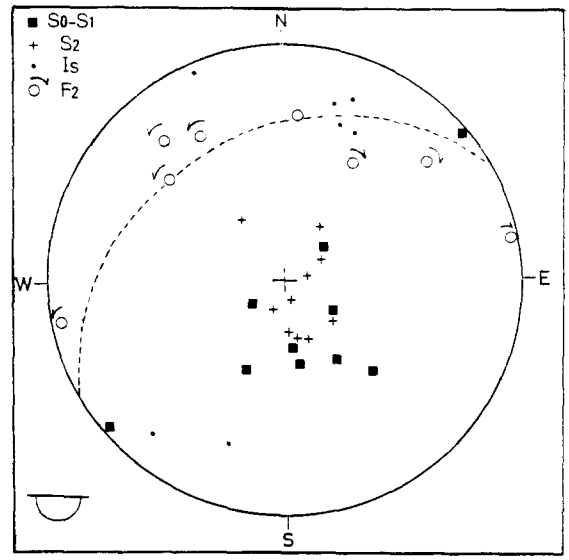


Fig. 15. Dispersion of the major $F_2$ fold axes and concentration of the stretching lineation (*ls*) in the NNE–SSW direction, Muscat nappes, Ruwi area. The dispersion of the fold axes in the $S_2$ plane is ascribed to the effect of shearing in the *ls* direction. The vergence of the folds (curved arrows) indicates thrusting towards the south.

dispersion of their axes in the $S_2$ plane (Fig. 15), responsible for the typical 'banana-shape' of some of them. The same shearing mechanism is also responsible for the reorientation of the axes of most minor $F_1$ and $F_2$ folds towards the stretching lineation.

## DISCUSSION AND CONCLUSIONS

Two main tectonic stages have been previously identified in the Oman obduction process: a high-temperature, intra-oceanic pre-obduction 'detachment', and a low-temperature, supracontinental gravity emplacement (Coleman 1981). Our structural observations provide a more precise insight on these events, and particularly on their kinematics. They also enable a third event to be identified: a HP–LT shearing episode at the innermost outcrop limit of the Arabian platform, as first reported by Michard *et al.* (1981) and Boudier & Michard (1981).

The connection between this epicontinental flat-lying shear zone (the Muscat nappes and NE-Saih Hatat metamorphics) and the obduction itself is not as straightforward as was supposed by the authors of the above papers. The Hawasina–Semail obduction lies tectonically upon the upper part of this shear zone (the Muscat nappes), with a major gap between them, both in fabric and metamorphic grade: the deformation in HP–LT conditions which is recorded within the Muscat nappes and the underlying metamorphics (the NE-Saih-Hatat) cannot be directly ascribed to the Hawasina–Semail emplacement which occurred under very low-grade conditions. On the contrary, it may be related to the thrusting of the Matrah peridotites onto this particular area of the Arabian margin. This slab of ultrabasites rests directly upon the Muscat nappes, south of Muscat

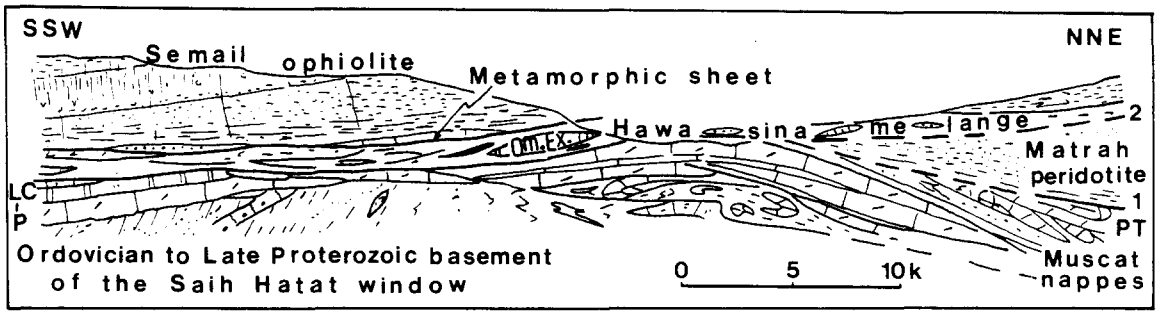


Fig. 16. Hypothetical tectonic sketch of the Oman obduction before the Late Maastrichtian transgression. 1, Basal thrust of the Matrah peridotite, probably contemporaneous with the Muscat and Saih Hatat HP–LT syntectonic metamorphism; 2 basal thrust of the Hawasina + Semail nappes, emplaced as a gravity driven complex; P to LC, Permian to Late Cretaceous limestones and Campanian–Early Maastrichtian marls (autochthon); PT, Permian and Triassic limestones (Muscat nappes).

(Fig. 8) and, like the nappes themselves, is overlain tectonically by the Hawasina mélange (Michard 1983). The thickness of the emerged massif is 3.5 km, measured perpendicular to the banding, but the actual thickness of the whole peridotite slab must be greater, as suggested by the strong positive gravity anomaly offshore (Manghnani & Coleman 1981). The ultrabasites, typified as 'basal' peridotites deformed in an intra-oceanic thrusting environment, would be the remains of a much thicker ophiolitic pile, submitted to tectonic and/or erosional thinning after its emplacement.

According to this hypothesis, two successive obductions, namely the Matrah and Semail obductions would have to be distinguished (Fig. 16), each one being characterized by a distinct structural and metamorphic signature. The earliest, the Matrah obduction, probably resulted from a synmetamorphic HP–LT shearing, carrying a slab of oceanic lithosphere southward upon the margin of the Arabian continent. This would be a post-Triassic, pre-Late Maestrichtian event (the age of emplacement of the epicontinental Muscat nappes is hypothetically related to this obduction). The latest obduction which is the classic Semail obduction, has the characteristics of a gravity-driven complex of nappes (Coleman 1981) carrrying ophiolites as well as slope-and-basin units onto a broad continental area. The direction of sliding was to the SW, slightly divergent at the scale of Oman as a whole. This was a Campanian–Maestrichtian event.

Both obductions involve basal peridotites already deformed in intra-oceanic thrusting conditions, with similar E–W lineations. The Semail obduction includes a typical transported HT metamorphic sole (lacking under the Matrah peridotites), which is the more complete signature of the intra-oceanic episode (pre-obduction detachment). This event is dated from 90 to 80 Ma (Ghent & Stout 1981). The relationship between the Semail obduction and the suggested Matrah obduction is still not clear. Is the epicontinental shearing a continuation of the intra-oceanic one (with a different direction), or not? We feel that the question needs more data to be answered, particularly a precise dating of the HP–LT event.

*Acknowledgements*—This work is part of the French project Nantes–Strasbourg in Oman, conducted under the authority of the Petroleum and Minerals Directory, Oman. It was supported by grants from the Centre National de la Recherche Scientifique and from Strasbourg University, and by a logistic assistance from Elf-Aquitaine-Exploration. We thank Dr. M. Quasim, Director of Petroleum and Minerals for his helpful welcome, and Dr. A. W. B. Siddans for linguistic and geological remarks. Equipe de Recherche Associée 887 (C.N.R.S.).

## REFERENCES

Bouchez, J. L. & Pêcher, A. 1981. The Himalayan Main central Thrust pile and its quartz-rich tectonites in central Nepal. *Tectonophysics* **78**, 23–50.

Boudier, F. & Coleman, R. G. 1981. Cross section through the peridotite in the Semail ophiolite. Southeastern Oman mountains. *J. geophys. Res.* **86**, 2573–2592.

Boudier, F. & Michard, A. 1981. Oman ophiolites: the quiet obduction of oceanic crust. *Terra cognita* **1**, 109–118.

Boudier, F., Nicolas, A. & Bouchez, J. L. 1982. Kinematics of oceanic thrusting and subduction from basal sections of ophiolites. *Nature, Lond.* **296**, 825–828.

Brookfield, M. E. 1977. The emplacement of giant ophiolite nappes. 1. Mesozoic–Cenozoic examples. *Tectonophysics* **37**, 247–303.

Coleman, R. G. 1971. Plate tectonic emplacement of upper mantle peridotites along continental edges. *J. geophys. Res.* **76**, 1212–1222.

Coleman, R. G. 1981. Tectonic setting for ophiolite obduction in Oman. *J. geophys. Res.* **86**, 2497–2508.

Dewey, J. F. 1976. Ophiolite obduction. *Tectonophysics* **31**, 93–120.

Elliott, D. 1976. The motion of thrust sheets. *J. geophys. Res.* **81**, 949–963.

Ghent, E. D. & Stout, M. Z. 1981. Metamorphism at the base of the Semail ophiolite. Southeastern Oman mountains. *J. geophys. Res.* **86**, 2557–2571.

Glennie, K. W., Boeuf, M. G. A., Clarke, M. W. H., Moody-Stuart, M., Pilaar, W. F. H. & Reinhardt, B. M. 1974. Geology of the Oman mountains. *Verh. K. Ned. geol.-mijnb. Genoot.* **31**, 1–423.

Glennie, K. W. 1977. Outline of the geology of Oman. *Mém. h. sér. Soc. géol. Fr.* **8**, 25–31.

Lippard, S. J. 1983. Cretaceous high pressure metamorphism in NE Oman and its relationship to subduction and ophiolite nappe emplacement. *J. geol. Soc. Lond.* **140**, 90–104.

Lovelock, P. E. R., Potter, T. L., Walsworth-Bell, E. B. & Wiemer, W. M. 1981. Ordovician rocks in Oman mountains: Amdeh formation. *Geologie Mijnb.* **60**, 487–495.

Malavieille, J., Etchecopar, A. & Burg, J. P. 1982. Analyse de la géométrie des zones abritées: simulation et application à des exemples naturels. *C.r. hebd. Séanc. Acad. Sci., Paris* **294**, 279–281.

Manghnani, M. H. & Coleman, R. G. 1981. Gravity profiles across the Semail ophiolite, Oman. *J. geophys. Res.* **86**, 2509–2525.

Michard, A. 1982. Contribution à la connaissance de la marge nord du Gondwana: une chaîne plissée paléozoïque, vraisemblablement hercynienne, en Oman. *C.r. hebd. Séanc. Acad. Sci., Paris* **295**, 1031–1036.

Michard, A. 1983. Les nappes de Mascate (Oman), rampe épicontinentale d'obduction à faciès schiste bleu, et la dualité apparente des ophiolites omanaises. *Sci. Géol. Bull., Strasbourg* **36**, 3–16.

Michard, A., Bouchez, J. L. & Misseri, M. 1981. Les nappes métamorphiques de Mascate, nouvel élément infra-ophiolitiqe en Oman. 1st. Europ Union Geosciences, Strasbourg. *Terra cognita* **1**, 19.

Michard, A., Bouchez, J. L. & Ouazzani-Touhami, M. 1982. Obduction related planar and linear fabrics, Oman. *Mitt. Geol. Inst. ETH Zürich Univ.* **239a**, 211–213.

Michard, A., Goffé, B. & Ouazzani-Touhami, M. 1983. Obduction related high pressure, low temperature metamorphism in upper crustal materials, Oman. *Terra. cognita* **3**, 187.

Misseri, M. 1982. Structures des massifs ophiolitiques de Canyon mountain (Oregon) et de Wadi Tayin (Oman): lithosphère d'arc insulaire; lithosphère océanique. Thèse 3e cycle, Nantes.

Nicolas, A. & Le Pichon, X. 1980. Thrusting of young lithosphere in subduction zones with special reference to structures in ophiolitic peridotites. *Earth Planet. Sci. Lett.* **46**, 397–406.

Parrot, J. F. & Whitechurch, H. 1978. Subduction antérieure au charriage Nord–Sud de la croûte téthysienne: facteur de métamorphisme de séries sédimentaires et volcaniques liées aux assemblages ophiolitiques syro-turcs, en schistes verts et amphibolites. *Rev. Géogr. phys. Géol. dyn.* **2**, 153–170.

Searle, M. P. & Malpas, J. 1981. Structure and metamorphism of rocks beneath the Semail ophiolite of Oman and their significance in ophiolite obduction. *Trans. R. Soc. Edinb.* **71**, 247–262.